Forced Convection in Asymmetric Wavy Channel

Dr. Ahmed Waheed Mustafa
University of Tikrit
Mechanical Engineering Department

Abstract

The effects of wavy wall in asymmetric two-dimensional channel on flow and heat transfer have investigated in this paper. The flow and temperature fields are studied numerically with different amplitude to channel length ratio and different number of waves. The laminar flow field is analyzed numerically by solving the steady, two-dimensional incompressible Navier-Stokes and energy equations. The Cartesian velocity components and pressure on a collocated (non-staggered) grid are used as dependent variables in the momentum equations, which discretized by finite volume method, body fitted coordinates are used to represent the complex wavy wall geometry accurately, and grid generation technique based on elliptic partial differential equations is employed. SIMPLE algorithm is used to adjust the velocity field to satisfy the conservation of mass. The range of Reynolds number is (Re = 50 - 500). The results show that at high amplitude to wave length ratio and high Reynolds number the wavy channel is an effective heat transfer device and the heat transfer enhancement increases with increases the number of waves. Good agreement with the published available data is obtained.

Keywords: Forced Convection, Wavy Channel, Finite Volume

الخلاصة

تأثيرات الجدار المتموج على الجريان وانتقال الحرارة في قناة غير متناظرة تم تحريه في هذة المقالة. حقل الجريان ودرجة الحرارة تم دراستة عدديا بنسب سعة موجة الى طول قناة وعدد موجات مختلفة. حقل الجريان الطباقي تم تحليلة عدديا بحل معادلات نافير ستوك والطاقة الثنائتي البعد وللحالة المستقرة.

مركبات السرع الدكارتية والضغط على شبكة متحدة الموقع استخدما كمتغيرات متعمدة في معادلة الزخم التي تم تقطيعها باستخدام طريقة الحجم المحدد. نظام تطابق الاحداثيات استخدم لتمثيل شكل القناة المعقد بشكل دقيق, تم توليد شبكة الحل العددي بحل معادلات تفاضلية جزئية بيضوية. خوازمية SIMPLE استخدمت لتحقيق حفظ الكتلة. مدى رقم رينولد هو (50-500) . النتائج بينت عند سعة الموجة العالية وعند رقم رينولد العالي فأن القناة تكن وسيلة فعالة لانتقال الحرارة وتحسين انتقال الحرارة يزداد عند زيادة عدد الموجات. توافق جيد تم الحصول علية مع النتائج المنشورة.

Nomenclature

G_1 Contravariant velocity in ζ direction

G_2 Contravariant velocity in η direction

H Dimensionless channel height

J Jacobian transformation

L Channel length (m)

n Number of waves

Nu Nusselt number

p Pressure (Pa)

P Dimensionless pressure

Pr Prandtl number

Re Reynolds number

S_ϕ Source term

U Dimensionless velocity in X-direction

U_∞ Inlet velocity (m)

V Dimensionless velocity in Y-direction

X Dimensionless axial coordinate

Y Dimensionless vertical coordinate

α, β, γ Dimensionless coordinate transformation parameters

Γ Dimensionless diffusion coefficient

λ Ratio of the wave amplitude to channel length

μ Viscosity (Pa.s)

ζ, η Dimensionless curvilinear coordinates

ρ Density (Kg/m^3)

ϕ Dimensionless dependent variable

1. Introduction

The wavy wall channel is employing for enhancing heat transfer in heat exchanger applications. Goldstein and Sparrow [1] were among the first to experimentally measure local and average heat transfer coefficients in a corrugated channel, in laminar, transitional and turbulent flow regimes. Their results showed secondary flows inside the triangular waves which resulted in as much as a 300% increase in the averaged heat transfer in turbulent regimes. Nishimura etc. [2] have investigated experimentally the flow pattern and mass transfer characteristics in symmetric wavy-walled channels at moderate Reynolds numbers (Re = 20–300). They considered two different wall shapes: sinusoidal walls and arc-shaped. They concluded that the characteristics of mass transfer for wavy-walled channels differ from those of a straight-walled channel when flow separation takes place.

The fluid flow and heat transfer through a periodic array of symmetric sinusoidal-shaped channels were studied numerically by Wang and Vanka [3], they observed that in steady flow regime, the average Nusselt numbers for the wavy wall channel were only slightly larger than those for parallel plate channel. However, in the transitional flow regime, the enhancement of heat transfer was by a factor of 2.5. Wang and Chen [4] analyzed numerically the flow and heat transfer in symmetric wavy channel; they used spline alternating-direction implicit (SADI) method. They found that the heat transfer enhancement is not significant at small amplitude wave length ratio. Bahaidarah etc. [5] studied heat and momentum transfer in both sinusoidal and arc-shaped channels. They predicted good heat transfer enhancement for some cases. The purpose of this study is to examine the effects of geometric parameters on the two-dimensional fluid flow and heat transfer characteristics in asymmetric wavy channels for different values of Reynolds numbers. The asymmetrical channel is represented by flat isothermal bottom wall and adiabatic wavy upper wall.

2. Mathematical Model

The basic flow configuration, under study, is shown in figure 1. The flow is considered to be two-dimensional, laminar, steady, constant fluid properties, and incompressible. The dimensionless continuity, momentum, and energy equations in Cartesian coordinates are given as

$$\frac{\partial U}{\partial X}+\frac{\partial V}{\partial Y}=0 \qquad (1)$$

$$\frac{\partial (U\phi)}{\partial X}+\frac{\partial (V\phi)}{\partial Y}=\frac{\partial}{\partial X}\left(\frac{1}{\Gamma}\frac{\partial \phi}{\partial X}\right)+\frac{\partial}{\partial Y}\left(\frac{1}{\Gamma}\frac{\partial \phi}{\partial Y}\right)+S_{\phi} \qquad (2)$$

Where the general dependent variable ϕ, the effective diffusion coefficient $1/\Gamma$, and the source term S_{ϕ} for momentum and energy conservation are defined as

$$\phi = \begin{bmatrix} U \\ V \\ \theta \end{bmatrix}, \quad \Gamma = \begin{bmatrix} \mathrm{Re} \\ \mathrm{Re} \\ \mathrm{Re}\,\mathrm{Pr} \end{bmatrix}, \quad S_\phi = \begin{bmatrix} -\dfrac{\partial P}{\partial X} \\ -\dfrac{\partial P}{\partial Y} \\ 0 \end{bmatrix} \tag{3}$$

These dimensionless equations are based on the following set of definitions, in which the lower-case symbols represent the physical (dimensional) quantities

$$(X,Y) = \frac{(x,y)}{L}, \quad (U,V) = \frac{(u,v)}{U_\infty}, P = \frac{p}{\rho U^2{}_\infty} \quad \theta = \frac{T - T_\infty}{T_w - T_\infty} \quad \mathrm{Re} = \frac{U_\infty L}{\nu}, \quad \mathrm{Pr} = \frac{\nu}{\alpha} \tag{4}$$

3. Wave Model

In order to simulate the wavy wall, a sinusoidal wave is used on the upper wall of the channel, the wave equation can be expressed as:-

$$Y = \lambda Sin(2\pi n X) + H \tag{5}$$

Where λ is the ratio of the wave amplitude to channel length, n is the number of the waves, and H is the dimensionless channel height.

4. Configuration and Boundary Conditions

The basic flow configuration, under study, is shown in figure 1. The boundary conditions used in the numerical solution are also illustrated in figure 1.

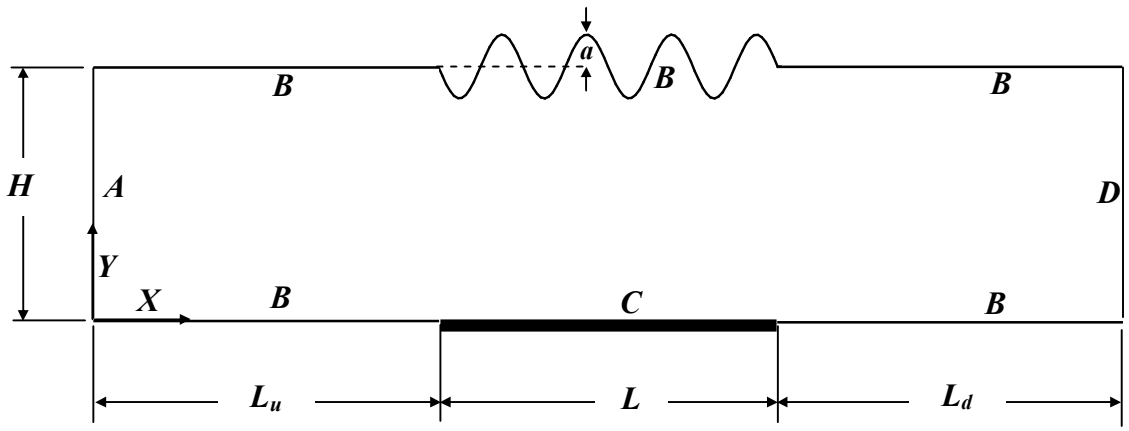

$(A)\quad U = 1,\ V = 0,\ \theta = 0,\ \dfrac{\partial P}{\partial X} = 0$ $\qquad$ $(B)\quad U = 0,\ V = 0,\ \dfrac{\partial \theta}{\partial Y} = 0,\ \dfrac{\partial P}{\partial Y} = 0$

$(C)\quad U = 0,\ V = 0,\ \theta = 1,\ \dfrac{\partial P}{\partial Y} = 0$ $\qquad$ $(D)\quad \dfrac{\partial U}{\partial X} = \dfrac{\partial V}{\partial X} = \dfrac{\partial \theta}{\partial X} = 0,\ P = 0$

Figure (1) Geometry and Boundary Conditions

5. Body Fitted Coordinates

The grid generation scheme developed by Thompson et al. [6], is used in the present study. In this method, the curvilinear coordinates are generated by solving the elliptic equations

$$\left.\begin{aligned}\alpha\frac{\partial^2 X}{\partial\varsigma^2}-2\gamma\frac{\partial^2 X}{\partial\varsigma\partial\eta}+\beta\frac{\partial^2 X}{\partial\eta^2}=0\\ \alpha\frac{\partial^2 Y}{\partial\varsigma^2}-2\gamma\frac{\partial^2 Y}{\partial\varsigma\partial\eta}+\beta\frac{\partial^2 Y}{\partial\eta^2}=0\end{aligned}\right\} \quad (6)$$

Where

$$\left.\begin{aligned}\alpha&=\left(\frac{\partial X}{\partial\eta}\right)^2+\left(\frac{\partial Y}{\partial\eta}\right)^2\\ \gamma&=\left(\frac{\partial X}{\partial\varsigma}\frac{\partial X}{\partial\eta}\right)+\left(\frac{\partial Y}{\partial\varsigma}\frac{\partial Y}{\partial\eta}\right)\\ \beta&=\left(\frac{\partial X}{\partial\varsigma}\right)^2+\left(\frac{\partial Y}{\partial\varsigma}\right)^2\end{aligned}\right\} \quad (7)$$

The grid generation for the wavy channel for number of control volume (260 X 30) is illustrated in figure 2.

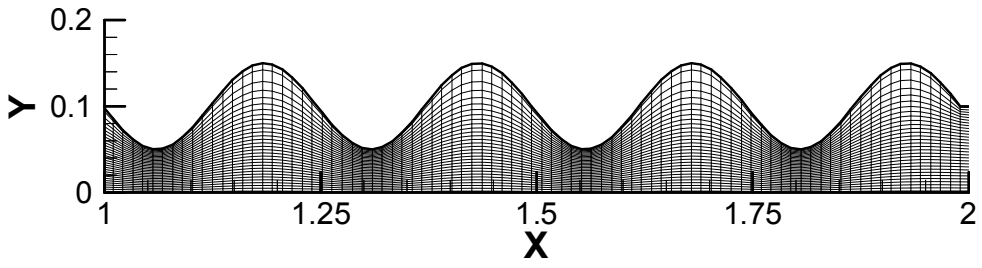

Figure (2) Gird Generation for λ = 0.03, n = 4 and number of control volumes MXN= 269X30

6. Transformation of the Governing Equations

Equation (2) can be transformed from physical domain to computational domain according to the following transformation:-

$$\left.\begin{aligned}\varsigma&=\varsigma(x,y)\\ \eta&=\eta(x,y)\end{aligned}\right\} \quad (8)$$

The final form of the transformed equation can be written as:-

$$\frac{\partial}{\partial\varsigma}(\phi G_1)+\frac{\partial}{\partial\eta}(\phi G_2)=\frac{\partial}{\partial\varsigma}\left(\frac{1}{\Gamma}J\alpha\frac{\partial\phi}{\partial\varsigma}\right)+\frac{\partial}{\partial\eta}\left(\frac{1}{\Gamma}J\beta\frac{\partial\phi}{\partial\eta}\right)+S_{\varsigma,\eta}+\frac{S_\phi}{J} \tag{9}$$

Where

$$\left.\begin{aligned} G_1 &= U\frac{\partial y}{\partial\eta}-V\frac{\partial x}{\partial\eta}, \\ G_2 &= V\frac{\partial x}{\partial\varsigma}-U\frac{\partial y}{\partial\varsigma}, \\ J &= 1/(\frac{\partial x}{\partial\varsigma}\frac{\partial y}{\partial\eta}-\frac{\partial y}{\partial\varsigma}\frac{\partial x}{\partial\eta}) \end{aligned}\right\} \tag{10}$$

And $S_{\zeta,\eta}$ is the source term due to the non-orthogonal and defined as: -

$$S_{\varsigma,\eta}=-\left(\frac{\partial}{\partial\eta}\left(\frac{J\gamma}{\Gamma}\frac{\partial\phi}{\partial\varsigma}\right)+\frac{\partial}{\partial\varsigma}\left(\frac{J\gamma}{\Gamma}\frac{\partial\phi}{\partial\eta}\right)\right) \tag{11}$$

7. Numerical Procedure

The Cartesian velocity components and pressure on a collocated (non-staggered) grid were used as dependent variables in the momentum and energy equations, which discretized by finite volume method, the convective terms were discretized by using hybrid scheme, while the diffusion terms were discretized by central scheme. Body fitted coordinates were used to represent the complex wavy wall geometry accurately, and grid generation technique based on elliptic partial differential equations is employed. **SIMPLE,** Patankar [7] algorithm was used to adjust the velocity field to satisfy the conservation of mass. Since all variables were stored in the center of the control volume, the interpolation method Rhie and Chow [8] was used to avoid the decoupling between velocity and pressure. The resulting set of discretization equations was solved iteratively using the line-by-line procedure which use the Tri-Diagonal Matrix Algorithm (TDMA). For further information, numerical details can be found in Ferziger and Peric [9].

8. Heat Transfer Calculation

The local Nusselt number can be calculated from

$$Nu=-\frac{\partial\theta}{\partial Y} \tag{12}$$

And the average Nusselt number on the lower wall of the channel is

$$Nua=-\int_0^1\frac{\partial\theta}{\partial Y}dX \tag{13}$$

9. Grid Independence

The table below shows the results of the average Nusselt number (Nua) obtained for the grid independence study for the case Re = 100, and λ = 0.03. A grid size of 260X41 (260 in X direction and 41 in Y direction) gives a grid independence solution.

Table 1 Grid Independence

Grid Size(MXN)	Nua
180X21	15.773
200X31	15.887
260X41	15.899
280X51	15.899

10. Validation

The numerical solution is validated by comparing the local Nusselt number along the wavy wall with the wavy channel that used by Wang and Chen [4]. The comparison is for the same channel of Wang and Chen [4], which has heating length of (From channel length = 3 to channel length = 15), six periods (n = 6), an amplitude-wave length ratio of 0.1, Reynolds number of 500, and a fluid Prandtl number of 6.93. Fully developed velocity profile was considered at the channel inlet. The comparison is shown in figure 3. As can be seen the agreement is good.

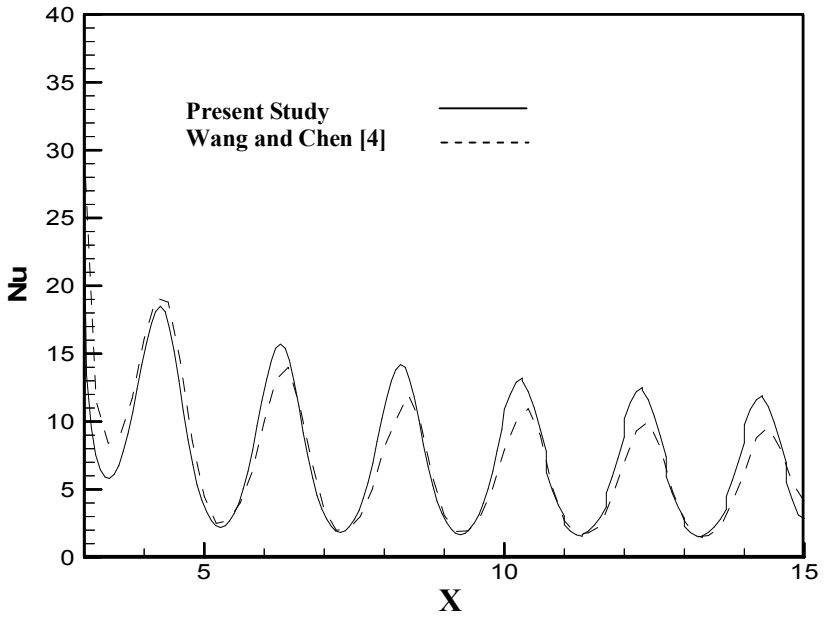

Figure (3) Comparison of Local Nusselt Number for the Present Work and for the Work of Wang and Chen [4]

11. Results

The numerical results are considered for the following case

H = 0.1

n = 2 – 8

λ = 0 – 0.05

An extra-length had to be added to the channel, upstream (L_u) and downstream (L_d) of the channel to represent the actual flow. Accuracy tests showed if $L_u = L_d = L$, the total heat transfer rate is insensible (with changes less than 1%) to any further doubling of L_u and L_d. Figure 4 shows that the local Nusselt number along the channel for different values of Reynolds numbers, the Nusselt number is higher in the converging section of each wave than in the diverging section. This is because the converging section has a higher average velocity which increases the heat transfer ratio.

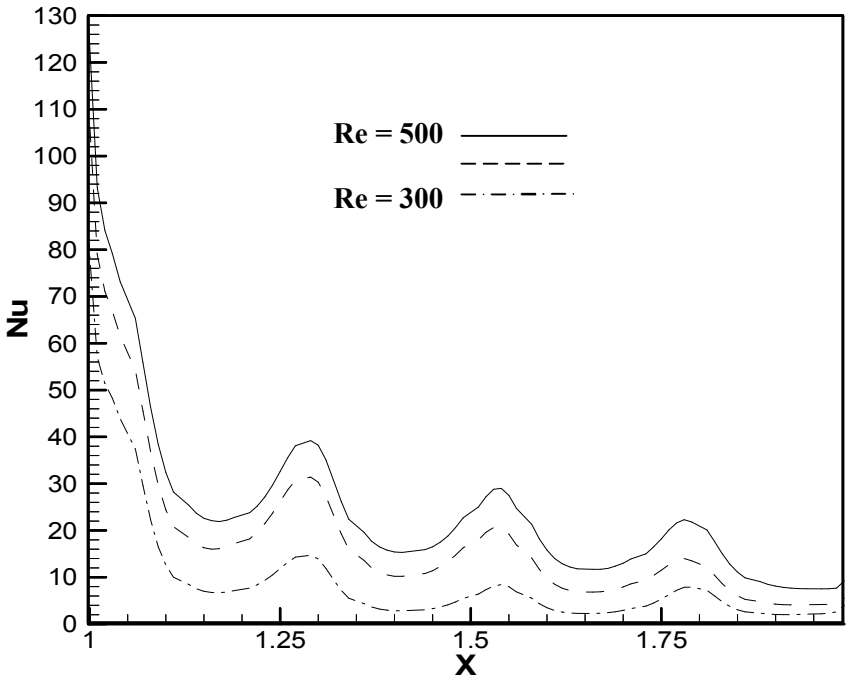

Figure (4) Local Nusselt Number along the Channel for λ = 0.05 and n = 4

Figure 5 shows the temperature fields for four different values of Reynolds number (Re = 50, 100, 300, and 500). As can be seen that the temperate gradients are increased near the lower wall as Reynolds numbers increased. This is clearly due to the effects of boundary layer flows near that wall, which increased the heat transfer rate from the channel walls.

Figure 6 show the variations in average Nusselt number with Reynolds number for different amplitude wavelength ratios at Pr = 0.71, and include the limiting case of a flat surface ($\lambda = 0$) for comparison purposes. The enhancement of heat transfer with Reynolds number and wavy wall is clear. At higher Reynolds number and higher amplitude to wave length ration the wavy channel is an effective heat transfer device. Also it can be seen from figure 7 that the heat transfer enhancement increases with increases the number of waves.

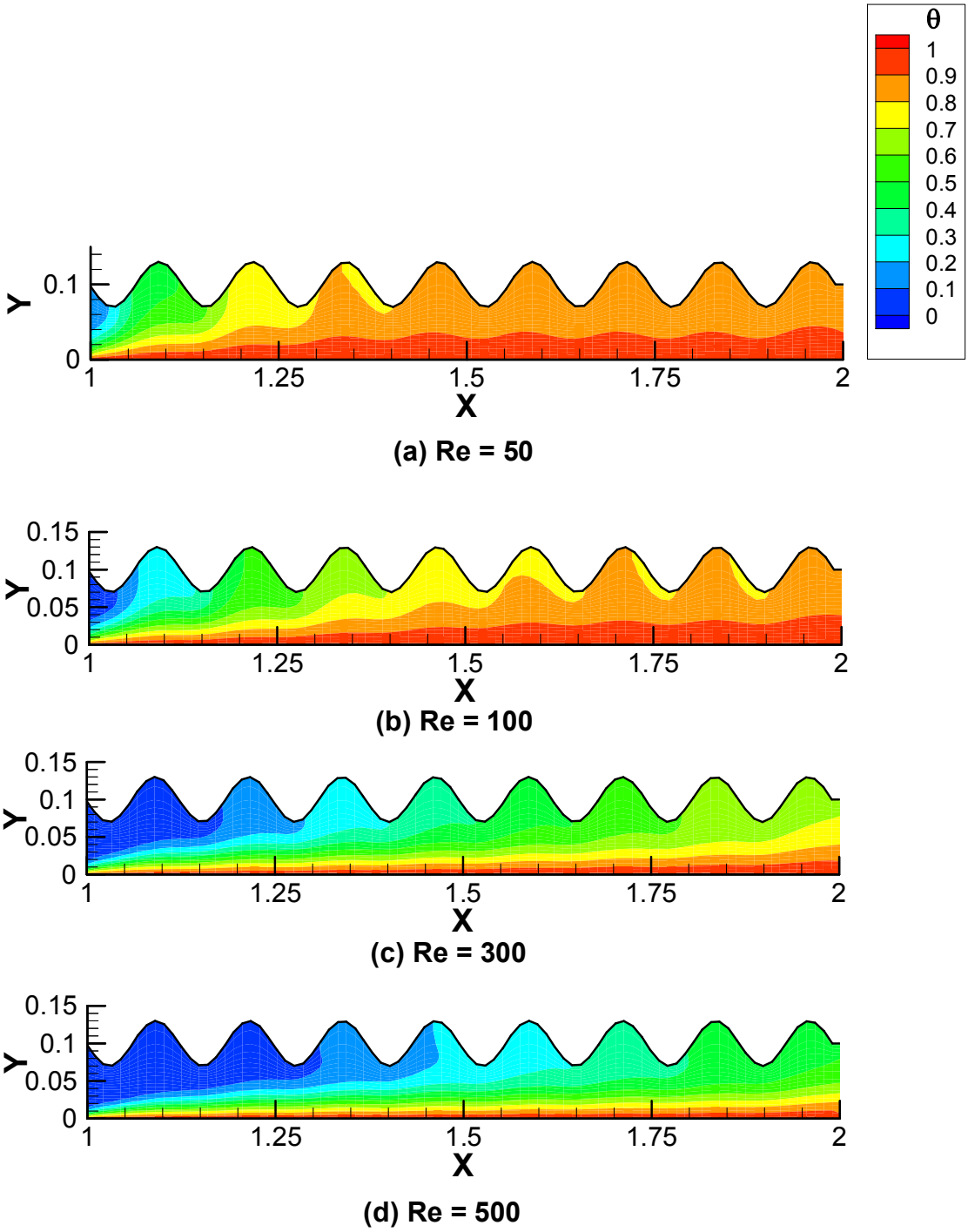

Figure (5) Temperature Contour for different values of Reynolds numbers and for λ =0.03, and n = 8.

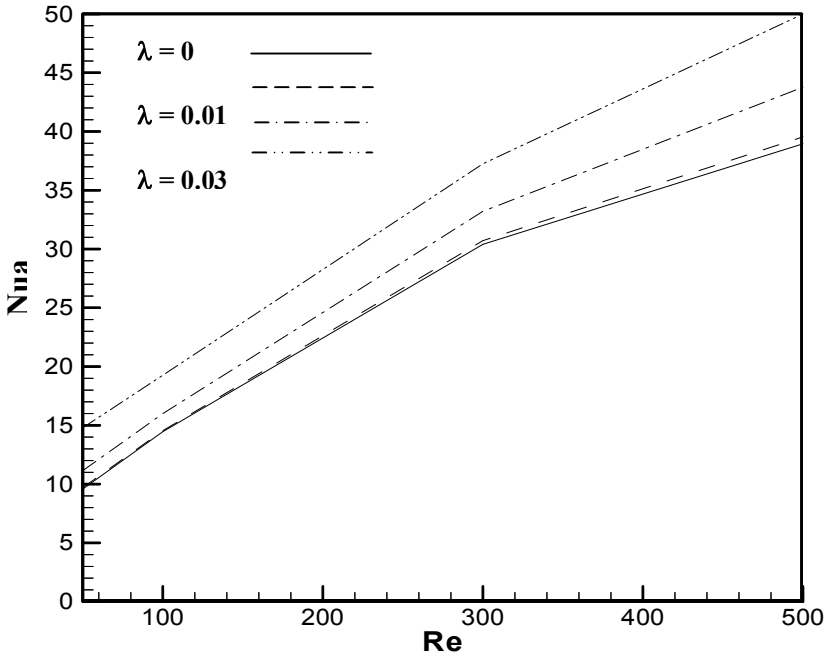

Figure (6) Average Nusselt number with Reynolds number for different values of wave amplitude, and for n = 4.

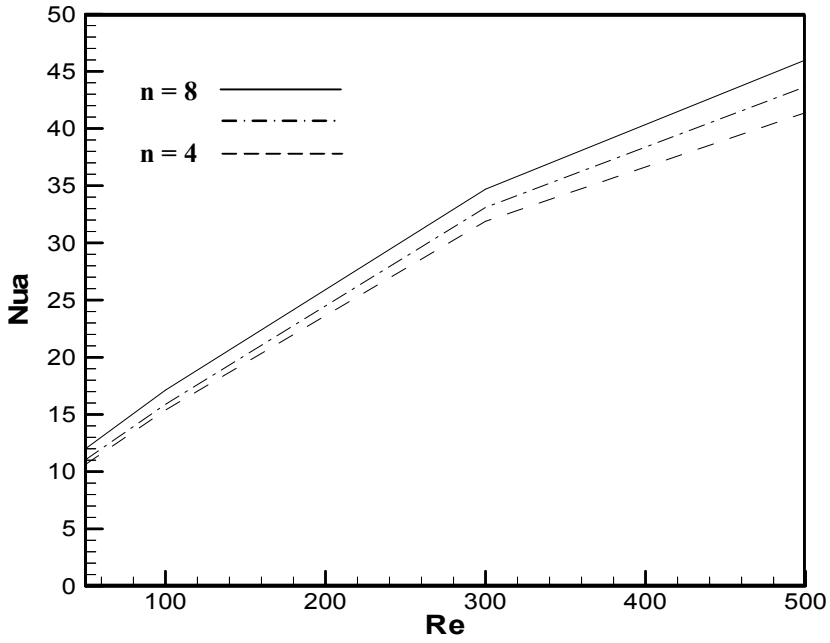

Figure (7) Average Nusselt number with Reynolds number for different values of wave number, and for λ = 0.03

12. Conclusions

The finite volume method with collocated grid is used to analyze the flow field and heat transfer in asymmetric wavy channel. The results show that at high amplitude to wave length ratio and high Reynolds number the wavy channel is an effective heat transfer device and the heat transfer enhancement increases with increases the number of waves.

13. References

1. Goldstein L. J. and Sparrow E. M. . Heat and mass transfer characteristics for flow in a corrugated wall channel. Journal of Heat Transfer, 99:187–195, 1977.
2. Nishimura T., Murakami S., Arakawa S., and Kawamura Y., Flow Observation and Mass Transfer Characteristics in Symmetrical Wavy-Walled Channels at Moderate Reynolds Numbers for Steady Flow, Int. J. Heat Mass Transfer, vol. 33, pp. 835–845, 1990.
3. Wang G. and Vanka. S. P. Convective heat transfer in periodic wavy passages. International Journal of Heat and Mass Transfer, 38(17):3219–3230, 1995.
4. Wang C. C and Chen. C. K. Forced convection in a wavy-wall channel. International Journal of Heat and Mass Transfer, 45:2587–2595, 2002.
5. Bahaidarah, H. M. S. Anand, N. K. and Chen. H. C. Numerical study of heat and momentum transfer in channels with wavy walls. Numerical Heat Transfer, Part A, 47:417–439, 2005.
6. Thompson, J.F., Warsi, Z.U.A., and Mastin, C.W., Numerical Grid Generation, Foundations and Applications. Elsevier, New York 1985.
7. Patankar, S.V., Numerical Heat Transfer and Fluid Flow, New York, Hemisphere Publishing Corporation, Taylor and Francis Group, 1980.
8. Rhie, C. M., and Chow, W. L., Numerical Study of the Turbulent Flow Past an Airfoil with Trailing Edge Separation, AIAA Journal, 1983,Vol.21, PP 1525-1532.
9. Ferziger, J.H. and Peric, M. Computational Methods for Fluid Dynamics, Springer 1996.